

Measuring the growth force of invasive plant cells using Flexure integrated Lab-on-a-Chip (FiLoC)

Mahmood Ghanbari¹, Muthukumaran Packirisamy^{1,*} and Anja Geitmann^{2,*}

¹Optical-Bio Microsystems Laboratory, Department of Mechanical and Industrial Engineering, Concordia University, Montreal, Québec H3G 1M8, Canada

²Department of Plant Science, Faculty of Agricultural and Environmental Sciences, McGill University, 21111 Lakeshore, Ste-Anne-de-Bellevue, Québec H9X 3V9, Canada

* Correspondence to: pmuthu@alcor.concordia.ca, anja.geitmann@mcgill.ca

Abstract

The pollen tube is a tip growing cell that is able to invade plant tissues in order to accomplish its function - the delivery of sperm cells to the ovule. The pistillar tissues through which the tube has to elongate represent a formidable mechanical obstacle, but it is unknown how much force the growing tube is able to exert, or how mechanical impedance affects its growth behavior. We quantified the invasive force of individual pollen tubes using a microfluidic lab-on-a-chip device featuring a microscopic cantilever. Using finite element method the maximum invasive growth force of the growing pollen tube was determined to be in the microNewton range. Real time monitoring revealed that contact with the mechanical obstacle caused a shift in the peak frequency characterizing the oscillatory behavior of the pollen tube growth rate. This suggests the presence of a feedback-based control mechanism with a mechanical regulatory component.

Keywords

Microsystems, Lab on Chip, Microfluidics, Microcantilevers, Cellular Interactions, Pollen Tube, Mechanobiology, Cellular Force

Introduction

Tip growing cells have the capacity to invade their surrounding substrate by forcefully penetrating their way through it. The purpose of this activity depends on the cell type and ranges from search for nutrients (fungal hyphae, root hairs) to creating connectivity between remote tissues (neurons) and delivery of cargo (pollen tubes). Overcoming mechanical impedance is a fundamental requirement for invasive growth and requires the cell to exert mechanical forces. Animal cells perform invasion using a cytoskeleton based mechanism whereas plant and fungal cells are thought to generate invasive forces by way of a hydroskeleton established through the turgor pressure¹.

A particularly efficient invasive cell whose successful penetrative behavior is required for fertilization is the pollen tube. The cellular

extension from the pollen grain is the delivery organ for the sperm cells in the flowering plants. The pollen tube has the purpose to invade the pistillar tissues and target an unfertilized ovule to deposit the sperm cells. This process results in fertilization of the female gametophyte and subsequent seed formation. The distance that the pollen tube has to overcome to reach an ovule can be as long as 30 cm and, depending on flower anatomy, multiple mechanical obstacles must be navigated to reach the target. Depending on the species these may include the cuticle covering the stigma, the apoplastic maze of the transmitting tissue filling the style, and/or the nucellus, a tissue surrounding the female gametophyte. The pollen tube softens these obstacles by secreting cell wall degrading enzymes or by inducing cell death in the invaded tissue². However, despite these chemically based efforts to soften the substrate, the pollen tube must generate a

considerable physical force to invade the different tissues³.

Pollen tube elongation is one of the fastest cellular growth processes known. In plants, cellular growth involves the stretching of the existing cell wall accompanied by assembly of new wall material⁴. In tip growing cells such as pollen tubes, this expansion of the cell surface is spatially confined to the extremity of the cell, the apex. This tip-focused morphogenesis occurs in other plant cells such as root hairs, but also in evolutionary very distant cells such as fungal hyphae. The principle of polar elongation and directed growth is also shared by nerve cells^{1,5,6}. The expansion of the pollen tube cell wall is driven by the turgor, the hydrostatic pressure that in walled cells can reach values in the range of MegaPascals. While turgor is the driving force⁷, regulation of growth speed and cell shaping resides in the cell wall^{8,9}. This notion is supported by measurements of the turgor using a pressure probe, that yielded no direct relation between the magnitude of turgor and the overall growth rate or between the instantaneous turgor and growth rate during the oscillatory growth in lily pollen tubes¹⁰. Inversely, the experimental manipulation of turgor pressure does affect the speed and dynamics of the oscillatory behavior⁸. Furthermore, without turgor, the pollen tube does not grow at all⁸. Clearly, both turgor and cell wall mechanical properties interact to regulate the growth behavior and several feedback models have been proposed to formalize this relationship^{11,12}. None of these models is able to explain how the pollen tube can grow and exert forces against the external environment, however. It is also poorly understood how exactly the invasive force of the pollen tube is regulated - whether through adjustment of the turgor or through modulation of the mechanical properties of the cell wall. A better understanding of the regulatory mechanism necessitates live cell observation of pollen tubes acting in their invasive capacity.

Quantifying the invasive force of a single cell requires a measuring device the dimension of which corresponds to that of the cell and whose dynamic range matches the forces to be measured¹. For

fungal hyphae the invasive force has been quantified by placing a strain gauge in front of the growing cell¹³, but this approach was challenging because of the relatively large size of the gauge and its limited sensitivity. The dilating force (directed side-wards) of pollen tubes was measured by letting the cells invade the narrow spaces made from elastic PDMS (Polydimethylsiloxane) material¹⁴. The known mechanical properties of this material allowed for the calculation of the forces that are exerted by the flanks of the tube to protect the tubular shape of the cell and hence the capacity of this catheter-like structure to transport a cargo in its lumen. To quantify the invasive force of the pollen tube, here we employed the strain gauge principle but using a micrometer sized, calibrated cantilever built into a Lab-on-Chip device. Moreover, we monitored the growth behavior of the pollen tube during interaction with the cantilever to understand how the tube regulates its invasive force upon interaction with an obstacle.

Materials and methods

Pollen culture

Camellia japonica pollen was collected from a plant growing in the Montreal Botanical Garden, dehydrated on silica gel for 2 h and stored at -20°C until use. Prior to each experiment, pollen was rehydrated in a humid chamber for at least 30 min without direct contact with liquid water. Pollen grains were suspended in a liquid growth medium containing 2.54 mM of $\text{Ca}(\text{NO}_3)_2 \cdot 4\text{H}_2\text{O}$, 1.62 mM of H_3BO_3 , 1 mM of KNO_3 , 0.8 of mM $\text{MgSO}_4 \cdot 7\text{H}_2\text{O}$ and 8% sucrose (w/v). Once the pollen grains started to germinate, the pollen suspension was introduced into the microfluidic chip.

Observation and analysis

Observation of growing pollen tubes in microfluidic channels was carried out using an inverted microscope (Nikon TE2000) equipped with a CCD camera (Roper fx). ImagePro (Media Cybernetics) and ImageJ 1.440 (National Institutes of Health, <http://rsb.info.nih.gov/ij>) software were used for data acquisition and analysis. Growth rate was

determined from the displacement of the pollen tube tip over time.

Design and fabrication

The PDMS-based Lab-on-Chip platform (Fig. 1) was designed to trap pollen grains, guide growing pollen tubes into a microchannel, and to present the elongating apex of the cell with a monolithically integrated, flexible PDMS microstructure with calibrated bending properties. The microfluidic

network consists of an inlet for injection of the pollen grain suspension, a distribution chamber to guide the pollen grains to the entrances of growth microchannels. Two identical growth microchannels (top and bottom) are incorporated for redundancy. A growth microchannel is designed to trap a pollen grain at its entrance and to guide the elongating pollen tube towards the microcantilever located at its end as developed previously¹⁵. Positioning of pollen grains occurs by laminar flow

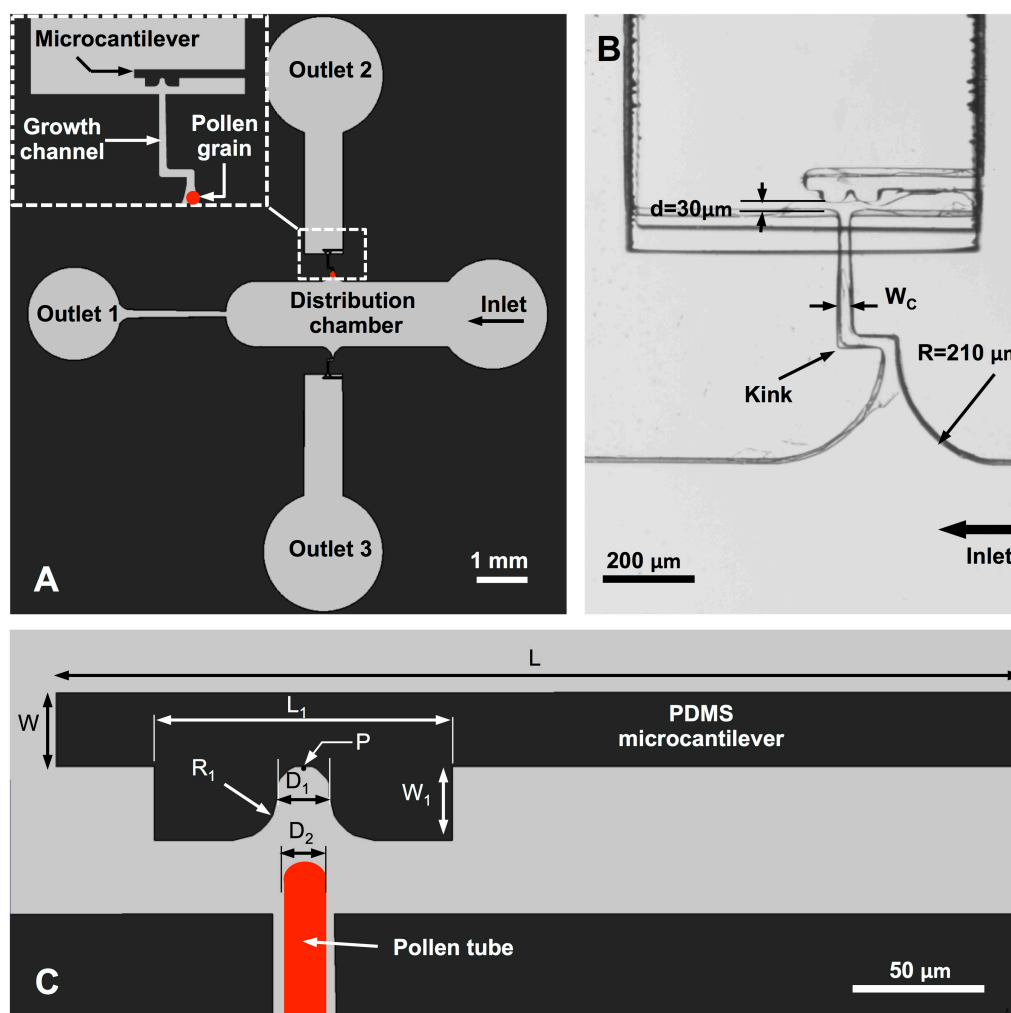


Figure 1. Flexure Integrated Lab-on-Chip (A) Schematic showing the geometry of the microfluidic network and the monolithically integrated PDMS microcantilever. Magnified view shows a pollen grain trapped at the entrance of a growth microchannel. (B) Brightfield micrograph showing the geometry of the microchannel and microcantilever. A kink is devised in the microchannel which prevents pollen grain backward displacement due to the reaction force applied by the growing pollen tube onto the distal portion and the grain. (C) Schematic showing the dimensions and geometry of the microcantilever. A curved notch was added to the cantilever to prevent the pollen tube tip from in-plane reorientation. The rounded corners of the notch entrance facilitate trapping of tube apex at the intended trapping point (P).

within the distribution channel based on previously optimized design of the distribution chamber (Fig. 1A)^{16,17}. Three outlets remove medium from the distribution chamber and from the ends of the microchannels. The distribution chamber outlet (Outlet 1) is large enough to also evacuate excess pollen grains. Outlets 2 and 3 enable fluid flow through the microchannels to ensure the pollen grain positioning. Pollen grains of *Camellia japonica* have a typical diameter of 50-60 μm . Therefore, the depth of the entire microfluidic network is set to be 80 μm in order to allow the grains to be transported freely by the fluid flow, without allowing their stacking in vertical direction. In order to avoid trapping multiple pollen grains at the entrances of the microchannels and to allow pollen tubes with a typical diameter of between 13-20 μm to enter these channels, the channel width (W_C) is set to 30 μm and the entrance of a microchannel is curved with a radius of 210 μm (Fig. 1B). The distance between the exit of the growth microchannel and the microcantilever (d) is kept as short as possible to prevent the pollen tube from passing above or below the microcantilever rather than pushing against it. Considering the limitations of the fabrication process, d was therefore set to 30 μm . To prevent push back through the interaction between the growing tube and the mechanical obstacle a kink consisting of two repeated 90° angles is incorporated into the microchannel thus anchoring the distal region of the tube (Fig. 1B). Furthermore, since the pollen tube easily changes its growth direction when encountering a mechanical obstacle, the cantilever is equipped with a curved notch with diameter (D_1) slightly bigger than the size of the average *Camellia* pollen tube diameter (D_2) that traps the pollen tube apex. The notch is incorporated into an appendix with Length L_1 , width W_1 added to the cantilever (Fig. 1C). This geometry prevents the pollen tube from in-plane reorientation and forces the cell to apply its maximum growth force onto the PDMS microcantilever (Fig. 1C). When the growing pollen tube touches the rounded corner ($R_1 = 17.5 \mu\text{m}$) of the entrance of the notch, it is guided into the notch and this increases the probability of trapping the pollen tube apex at the intended

location (point P). This ensures that the pollen tube applies its growth force fully onto the microcantilever rather than sliding along its surface.

For the design of the PDMS microcantilever the following considerations were made to establish its length (L) and width (W): 1) The dynamic range of cantilever deflection should be in the expected range of 1-15 μN , based on previously published values for the dilation force of *Camellia* pollen tubes and the invasive force of fungal hyphae^{13,14}. 2) The aspect ratio (L/W) had to be such that snapping of the cantilever to the top or bottom layer during the fabrication process is avoided. L was therefore chosen to be 400 μm and W 30 μm . The length (L_1) and width (W_1) of the appendix and diameter of the curved notch (D_1) were selected as 120 μm , 30 μm and 25 μm , respectively.

Multi-layer soft lithography was used for monolithical integration of the microcantilever within the microfluidic network consisting of three PDMS layers. The cantilever and microfluidic network pattern are fabricated as a thin PDMS structural layer (80 μm thick) that is sandwiched between a top and a bottom layer to create an enclosed microfluidic network. The bottom layer is a thick PDMS layer, whereas the top layer is 80 μm thin. Both are patterned to contain cavities to release the microcantilever for free in-plane deflection. The top layer is bonded to a glass cover slip (100 μm thick). The combined thickness of the top layer and glass cover slip (180 μm thick) allows us to use high resolution imaging and also makes the LOC compatible with confocal microscopy that might be used for fluorescence imaging in future experiments.

For fabrication, a photoresist layer (SU8-2075 negative photoresist; MicroChem Corp) was spin coated on the surface of a 4 inch silicon wafer (Fig. 2A) and patterned using conventional lithography process (Fig. 2B). Curing agent and PDMS prepolymer (Sylgard 184 silicone elastomer, Dow Corning Corporation, Midland, USA) mixed at a weight ratio of 1:10 was poured onto the SU-8/Silicone mold (Fig. 2C). To remove excess PDMS

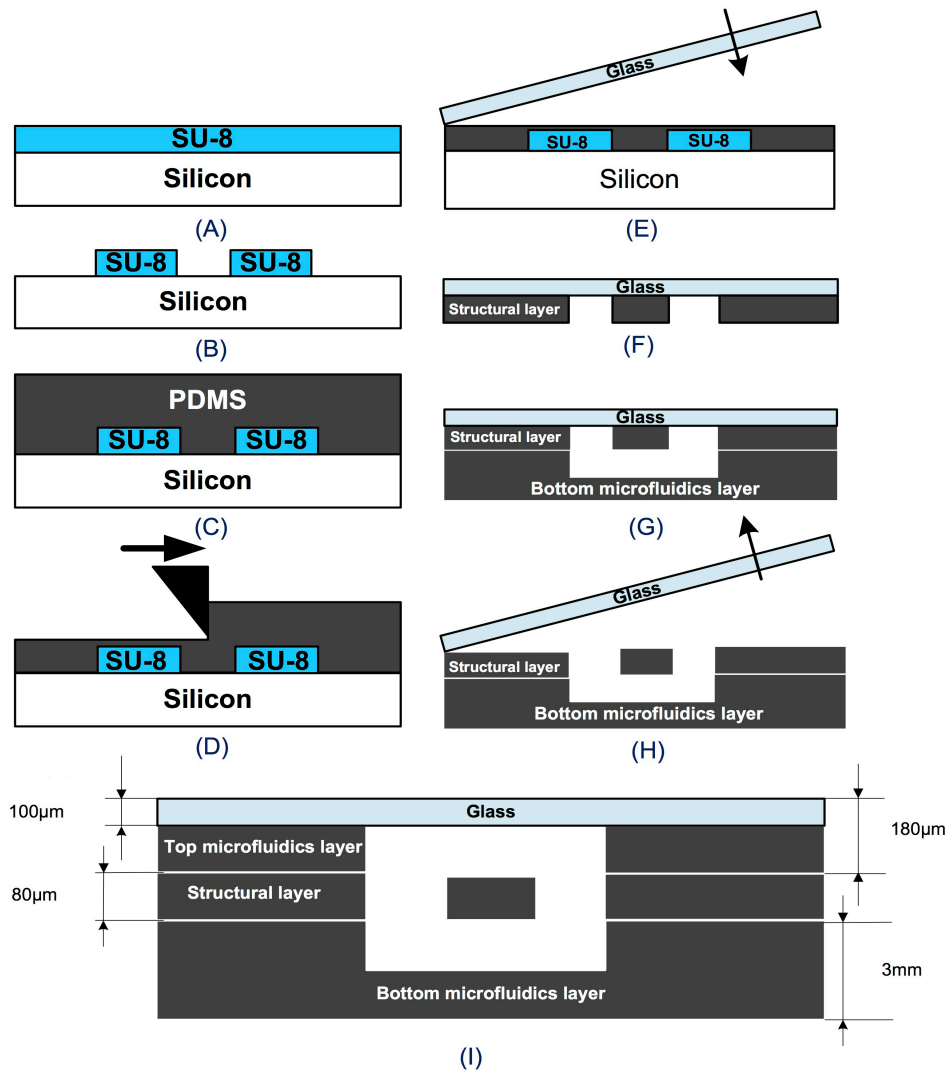


Figure 2. Schematic of the multi-layer fabrication processes developed for the fabrication of LOC platform. (A) An SU-8 layer is spin coated on the surface of a 4 inch silicon wafer. (B) SU-8 layer is patterned using lithography process to make a mold. (C) PDMS is poured onto the mold. (D) A blade is traversed above the substrate surface in order to remove excess PDMS on the surface of SU-8 features. (E) A glass slide is placed on the PDMS surface and loaded using a clamp. (F) After backing in an oven, the thin PDMS structural layer is peeled off from the mold using the glass slide and (G) bonded to the bottom

on the surface of SU-8 features, a blade was used to traverse the substrate surface while maintaining contact with the top surface of the photoresist layer (Fig. 2D). A thin film of PDMS (less than 5 µm thick) remains on the surface of photoresist region after this step. Subsequently, the mixture was completely degassed in the desiccator to get rid of the bubbles. Next, a glass slide was placed on the PDMS surface (Fig. 2E) and loaded using a clamp for curing inside an oven at 65°C for 4h. Using the

glass slide, the thin PDMS structural layer was peeled off from the mold (Fig. 2F) and bonded to the bottom microfluidics layer, which was fabricated by replica molding technique. Bonding was performed after oxygen plasma treatment for 30 sec (Harrick Plasma PDC-001) and microscopic alignment (Fig. 2G). Then, the glass slide was peeled off (Fig. 2H), the inlet and outlets were punched, and the top microfluidics layer was bonded to the sandwich layer using oxygen plasma treatment (Fig. 2I).

Results

The invasive force of a growing *Camellia* pollen tube is within the dynamic range of the PDMS microcantilever

To assess the force a growing pollen tube can exert, we designed a microscopic cantilever with a defined bending constant against which the cell would push. To this end a PDMS-based Lab-on-Chip platform (Fig. 1) was designed to trap pollen grains, guide growing pollen tubes into a microchannel, and to present the elongating apex of the cell with a monolithically integrated, flexible PDMS microstructure (Flexure Integrated Lab-on-a-Chip, FiLoC). A multi-layered fabrication process was necessary to ascertain free movement of the cantilever (Fig. 2). The position of the microcantilever was at 500 μm from the microchannel entrance, since at this length the pollen tube has typically reached its maximal growth rate.

To test the growth force of pollen tubes, ungerminated pollen grains of the species *Camellia* suspended in growth medium were injected into the microdevice. The optimal injection velocity to ensure stable positioning of pollen grains at the entrances of the microchannels had been established to be 0.01 m/s. Since continuous medium fluid flow would deform the cantilever and thus lead to an overestimation of the pollen tube growth force, medium flow was stopped once the grains were positioned. Pollen tubes usually formed within 30 min after positioning of the grains. Once a pollen tube had grown through the microchannel and entered the test chamber it pushed against the microcantilever (Fig. 3). In successful experiments the pollen tube touched the microcantilever at the notch entrance (point A in Fig. 3A), slipped into the notch (Fig. 3B), and then bent the cantilever (Fig. 3C). After an initial bending, the pollen tube sometimes stopped for few minutes before resuming its growth. Growth then proceeded until the growth

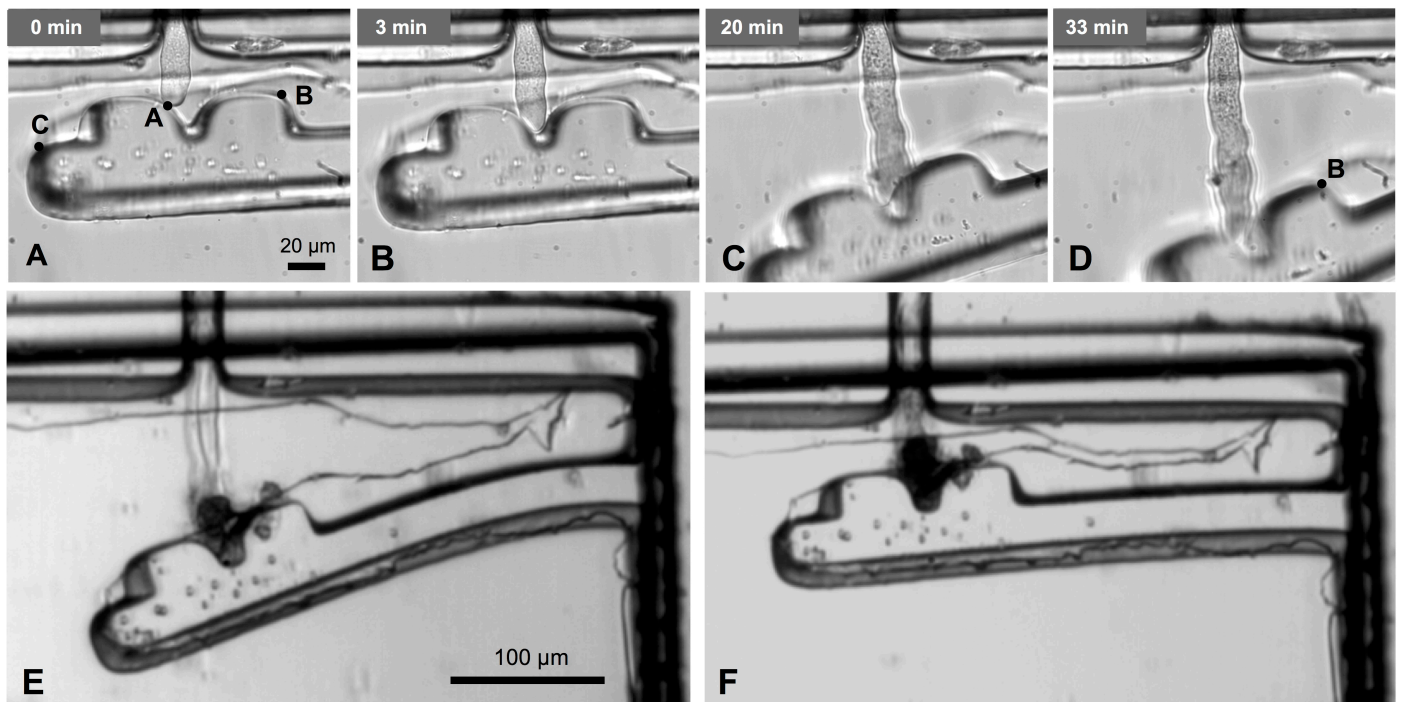


Figure 3. Time lapse image series of the pollen tube behavior during interaction with the microcantilever. (A) The pollen tube touches the microcantilever at point A on the rounded corner. (B) The pollen tube tip is guided into the notch by the rounded corner of the notch entrance. (C) The pollen tube continues its growth toward the intended trap point while applying its growth force against the cantilever. (D) Pollen tube growth is stopped, and after 6 minutes the tube resumes its growth and bends the cantilever further until maximum deflection is reached. (E) The pollen tube bursts and cantilever

force was not sufficient to displace the cantilever further (Fig. 3D). This maximum cantilever displacement corresponded to the maximum growth force the pollen tube was able to exert. Occasionally, this growth stall was eventually followed by the tube bursting (Fig. 3E) upon which the cantilever returned to its original position (Fig. 3F). In the example shown in Fig. 3 the deflection of the cantilever of point B was $58\ \mu\text{m}$ for this point which corresponds to a deflection of $118\ \mu\text{m}$ of the cantilever tip (Point C).

Experimental determination of the Young's Modulus of PDMS

To determine the pollen tube growth force based on the deflection of the microcantilever the bending constant of the latter had to be identified which in turn necessitates quantitative information on the Young's modulus of the PDMS material used here. Since the Young's modulus of the thin PDMS layer is dependent on the thickness of the layer and the fabrication process¹⁸, we did not rely on published material properties but measured these for the material used here. To do so a precision balance method was employed to quantify the Young's modulus of PDMS from the microcantilever stiffness¹⁹. A PDMS microcantilever fabricated as described above was bonded to a thick PDMS layer for mechanical stability and mounted horizontally on a micro positioner (ULTRAlign™ Metric Linear 3 Axis Stag, with resolution of $1\ \mu\text{m}$) (Fig. 4). Since the sensitivity of the precision balance method was

not sufficient to measure the in-plane stiffness of the cantilever, the cantilever stiffness in the normal direction was quantified as the PDMS beam has a higher bending constant in that direction due to geometry. Since PDMS is an isotropic material the obtained Young's modulus applies equally to the horizontal direction.

The microcantilever was lowered gradually such that comes in contact with the glass plate placed on the balance at $200\ \mu\text{m}$ away from the cantilever's support. The force applied by the microcantilever to the glass plate is directly transferred to the balance. The deflection of the cantilever was considered to be equal to the movement of the micro positioner. To quantify the stiffness of the microcantilever the forces (F) needed for the deflections (δ) of $15\ \mu\text{m}$, $30\ \mu\text{m}$, $45\ \mu\text{m}$, $60\ \mu\text{m}$ of the microcantilever were measured and linear regression was used to determine the beam stiffness (K) using $F=K\delta$ to be $0.35\ \mu\text{N}/\mu\text{m}$. The force-deflection diagram of the microcantilever confirms the linear behavior of the PDMS microcantilever even for large deflections (Fig. 4C). The elastic modulus of PDMS (E) was then calculated from the deflection equation of the beam $K = \frac{3EI}{L^3}$ to be $E = 750\ \text{kPa}$, where I and L are the moment of inertia and distance of the applied force from the cantilever support, respectively. This value is close to the value reported for the Young's modulus of thin PDMS layers^{18,19}.

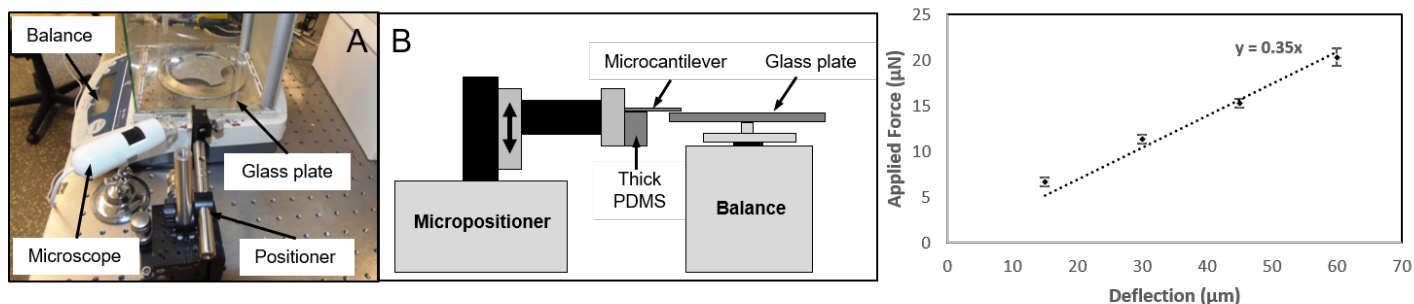


Figure 4. Experimental quantification of the beam stiffness of a PDMS cantilever. Photograph (A) and schematic diagram (B) of the precision balance setup used to determine the bending behavior of the PDMS microcantilever. (C) The force vs. deflection diagram of microcantilever. Error bars represent the standard deviation ($n=3$). Linear regression is used to estimate the beam stiffness, which is the slope of this line.

Quantification of pollen tube invasive growth force using Finite Element Modeling

To determine the pollen tube growth force based on the deflection of the microcantilever finite element modeling (FEM) was used. Because of the buckling behavior of the pollen tube once it exerts force against the cantilever (Fig. 5) it is assumed that the pollen tube exerts a point force (F) at contact angle θ with respect to the original position of the cantilever at contact point I (Fig. 5A). The microcantilever was modeled as 3D structure with

the dimensions mentioned in the Design and Fabrication section (Fig. 5). The Young's modulus of $E=750$ kPa determined by the precision balance method and the Poisson's ratio of $\nu=0.45$ were used to characterize the PDMS material¹⁹. As the boundary condition for FEM analysis, the bottom surface of the microcantilever (MNLK surface) represented the fixed support. A point force with angle θ with respect to the horizontal direction was applied to the variable contact point of the pollen tube and PDMS microcantilever. For each pollen

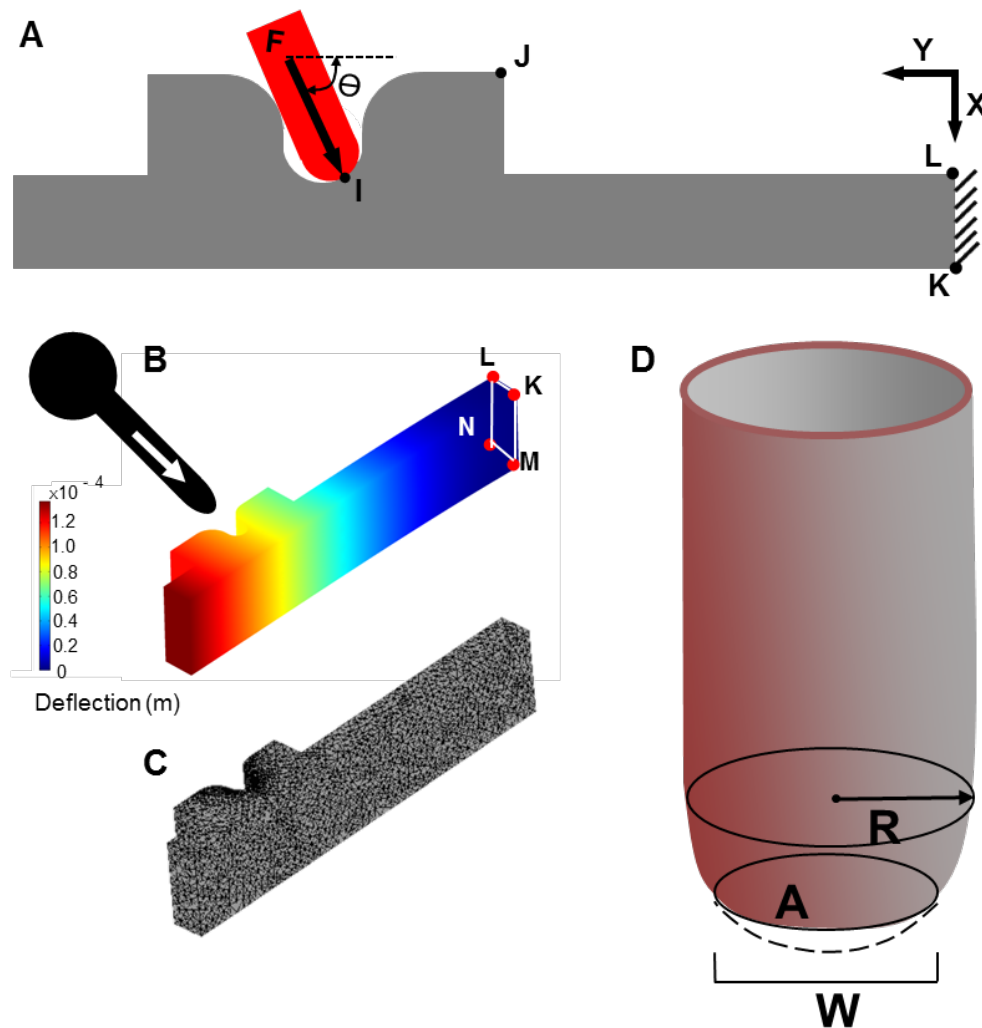


Figure 5. Geometry of the interaction between pollen tube and microcantilever. (A) Simplified schematic view of the interaction between an elongating pollen tube and PDMS microcantilever. (B) 3D view of microcantilever deflection at $F= 1.5 \mu\text{N}$, $\theta=80^\circ$ obtained using COMSOL Multiphysics 3.5 software. The color code represents the deflection of the PDMS microcantilever at the tip. (C) Mesh structure of the FE model. (D) Estimation of contact area A between pollen tube apex and PDMS microcantilever using width W of the flattened spherical cap as observed from micrographs.

tube the angle θ and the maximum deflection of the cantilever were determined. Only *bona fide* maximum force measurements were used. Pollen tubes that slipped above or below the cantilever, or pollen tubes that burst without prior stall were monitored for kinetic studies (see below) but not used for calculation of the average maximum point force. The average of the maximum force measurements was 1.5 μN (based on two cells displaying *bona fide* stalling behavior).

Based on this point force and on the area of the pollen tube apex in contact with the PDMS microcantilever, the effective pressure exerted by the elongating pollen tube onto PDMS microcantilever was determined. Since at maximum cantilever deflection the tube apex was obscured by the top edges of the notch wall, the area of contact of pollen tube with the microcantilever could not be visualized clearly. Therefore, the contact area was estimated at the moment the pollen tube touched the microcantilever and started deflecting it. During pressure exertion the pollen tube apex flattened slightly within a few seconds of contact. Therefore, contact area (A) was calculated with CAD software using the flattened width of the pollen tube tip (W) and angle at which tube hit the cantilever (Fig. 5D). For the tube shown in Fig. 3 dividing the maximum force (1.5 μN) by the calculated contact area A (12.5 μm^2) the maximum pressure exerted by the elongating pollen tube was determined to be 0.12 MPa.

Interaction with a mechanical obstacle affects pollen tube growth dynamics

Similar to many other plant species, pollen tubes of *Camellia* display an oscillatory growth pattern²⁰. In previous studies this oscillatory pattern has been manipulated experimentally to understand the mechanism regulating this growth dynamics (for a review see Kroeger and Geitmann¹¹). It has been hypothesized that this oscillatory behavior facilitates invasive growth akin to a sledge hammer^{1,21}. However, proof for this functional role is lacking. The concept would gain significant support if it were possible to demonstrate that the

magnitude of external mechanical impedance fed back onto the growth behavior of the tube. In other words, a change in oscillation frequency upon exposure to a mechanical obstacle would indicate that the pollen tube adapts to the magnitude of substrate stiffness. In order to analyze the effect of an external mechanical obstacle on pollen tube growth dynamics, the oscillation frequency before and during the contact with the microcantilever was analyzed. Before contacting the cantilever the pollen tube shown in Fig. 6A displayed growth rate changes oscillating between 4 and 19 $\mu\text{m}/\text{min}$ with the average being 11.3 $\mu\text{m}/\text{min}$. Upon first contact with the cantilever, this growth rate decreased by an average of 44% to 6.3 $\mu\text{m}/\text{min}$ (with min/max rates between 1.7 $\mu\text{m}/\text{min}$ and 12.7 $\mu\text{m}/\text{min}$). During the subsequent elongation of the tube while in contact with the microcantilever the average growth rate remained constant despite the increasing mechanical impedance created by the increasing cantilever deflection.

It is difficult to identify the frequency components only by evaluating the original signal. Therefore, to obtain discrete data, the time domain signal was converted to the frequency domain using discrete Fourier transform (DFT) in order to detect the peak frequency of oscillation. DFT of the signal is calculated using the fast Fourier transform (FFT) algorithm⁸. Even though the DFT analysis provides dominant frequencies that exist, power spectral density (PSD) was also estimated to eliminate the effects of randomness of the response. PSD was then applied to obtain waveform reflecting the power of each frequency components associated with the oscillatory growth in samples in which the duration of oscillatory growth in contact with the cantilever was sufficiently long for analysis. Both DFT and PSD of signals revealed that the interaction with the cantilever resulted in the same dominant frequencies of 40mHz and 12mHz with a typical reduction in the magnitude of the dominant peak frequencies by a factor of three (Fig. 6 B,C). In other words, the period of the principal oscillation signal increased threefold. In order to ascertain the main frequencies and remove ripples frequencies, three

different PSD windowing functions, namely, Kasier, Hamming and Chebyshev were used and were found to yield similar results (Fig. 6 D,E). The frequency of the growth behavior was therefore clearly affected by exposure to the mechanical obstacle.

Discussion

Invasive growth is a trait of fundamental importance that enables certain cell types to accomplish their respective functions. The purpose of invasive growth can range from the creation of communication highways over long distances (neurons) to exploring water and nutrient providing

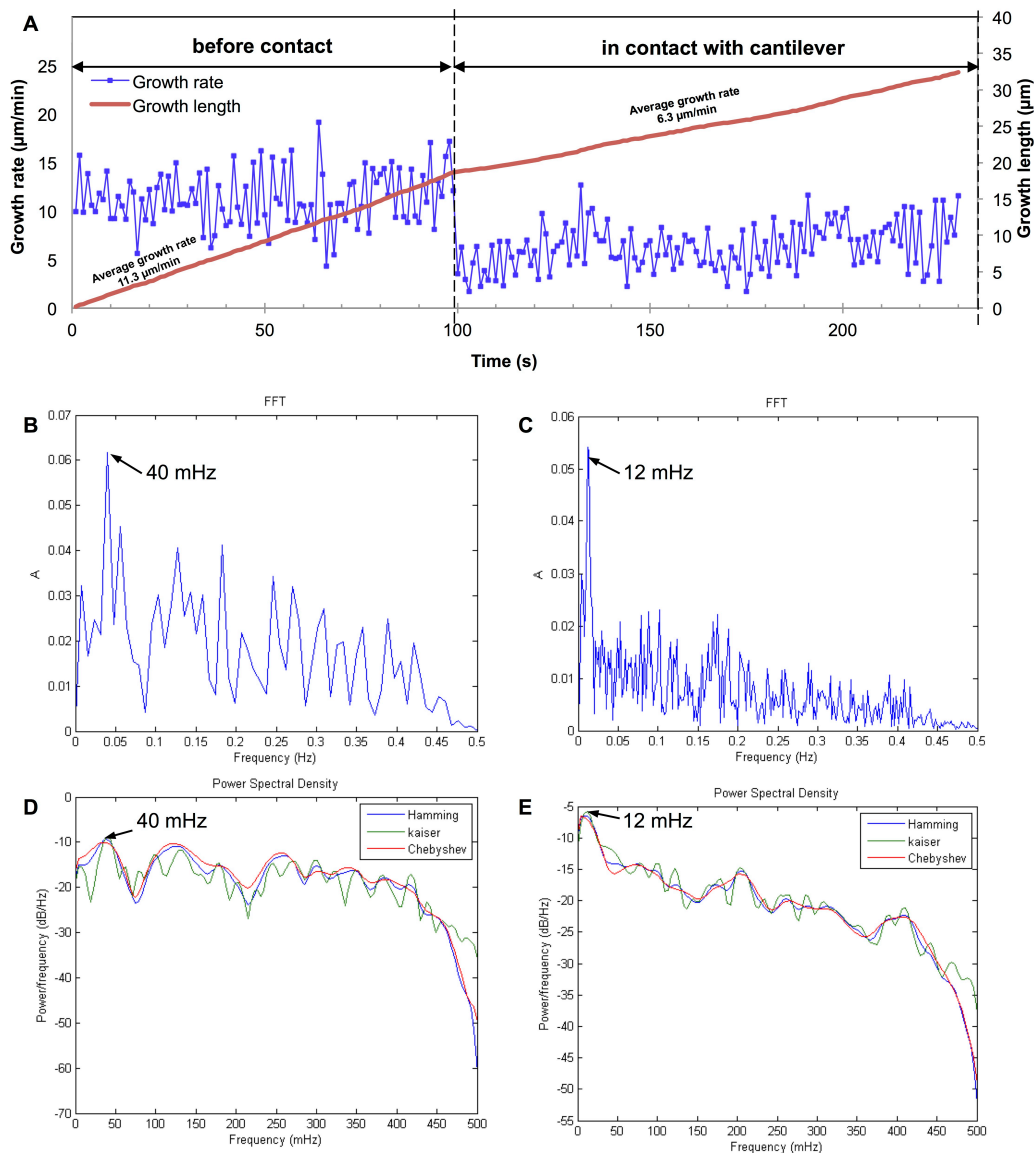


Figure 6. Effect of mechanical obstacle on pollen tube growth dynamics (A) Pollen tube growth rate and tube length before contact and during contact with the microcantilever. The average growth rate is reduced by 44% from 11.3 $\mu\text{m}/\text{min}$ to 6.3 $\mu\text{m}/\text{min}$ after contact with the microcantilever. The change is sudden and the average growth rate is maintained despite increasing bending of the cantilever. (B,C) FFT analysis on time-series data of sample *Camellia* pollen tubes growth rate (sample rate = 1s) before (B) and during (C) contact with the microcantilever. Peak frequencies are marked by arrows. (D,E) PSD analysis on time-series data shown in B and C, respectively.

substrates (fungal hyphae, root hairs) or implementation of architectural design strategies (sclerenchyma fibers). Pollen tubes practice invasive growth to accomplish the delivery function that is fundamental for reproduction in the flowering plants - the conveyance of the sperm cells. The TipChip enabled us to determine that the invasive growth force of an elongating pollen tube is approximately 1.5 μN . This is comparable to the 1.4 μN reported for hyphal invasive growth force determined by using a strain gauge¹³. However, given that the size of the fungal hypha used for that study has a much smaller diameter than a *Camellia* pollen tube, almost the same amount of force detected by the strain gauge translates into a much higher turgor pressure in the hypha. This is consistent with the fact that fungal structures can display pressures of up to 8 MPa²² whereas plant cell pressures are typically below 1 MPa.

If the hypothesis is correct that any growth force exerted by the elongating pollen tube against the microcantilever is generated by the internal turgor pressure, the maximum invasive pressure should not exceed this pressure. Our experiments showed that a maximum pressure of 0.12 MPa is exerted on the PDMS microcantilever by the elongating pollen tube before elongation stalls. This is consistent with the magnitude of pollen tube turgor pressure measured in growing pollen tubes of between 0.1-0.4 MPa¹⁰. Although these measurements were conducted in a different species, lily, the dimensions of lily and camellia pollen tubes and their *in vitro* growth rates are similar thus supporting the notion that the respective values for turgor pressure might be in the same range. Moreover, the calculated value of 0.12 MPa for the invasive pressure used by the *Camellia* pollen tube is consistent with the pressure value that had been determined earlier to act as dilating forces in pollen tubes of the same species. By letting tubes growth through elastic, slit-shaped openings¹⁴, estimated that a pressure of 0.15 MPa is exerted to dilate the microscopic opening. Dilation is crucial to enable the pollen tube to ensure the passage of the sperm cells inside the tube despite the presence of lateral compressive forces.

Remarkably, the pollen tube responds to the initial contact with the cantilever in rather drastic manner by a sudden drop in growth rate and a sudden shift in oscillation frequency towards lower values. If these responses were simply mechanically induced they would be expected to appear gradually and to increase in magnitude with increasing deflection of the cantilever. However, instead both phenomena, frequency shift and drop in growth rate are abrupt. Even more intriguing, they are not dose-dependent since they do not become more pronounced despite the increasing mechanical impedance due to cantilever deflection. Several conclusions can be drawn from these findings: Firstly, the pollen tube seems to sense when it contacts the surface of the obstacle and responds immediately. This is consistent with earlier observations of a reduction in pollen tube growth rate upon contact with a physical obstacle¹⁴. Secondly, the pollen tube is able to adjust to a higher impedance by modifying the force it exerts. The ability to sense the geometry and mechanics of its environment is very poorly understood in pollen tubes and no sensing mechanism has been identified at molecular level. The finding is consistent with other experimental evidence, however, for example with the fact that depending on the species pollen tubes avoid or seek out stiffer substrate when given a choice. Pollen tubes from *Arabidopsis* generally prefer an agarose stiffened medium compared to a liquid one, whereas pollen tubes of poppy show preference for a softer substrate³. When growing through obliquely angled microgaps, the growth rate drops initially, but not continuously¹⁴. Pollen tubes are hypothesized to possess mechanosensitive calcium channels in their apical membranes²³ which could fulfill the function of perceiving the deformation of the tip when it encounters an obstacle. No direct molecular evidence to support this notion is available so far, but the recent discovery of a pollen-expressed mechanosensitive channel involved in osmoregulation is encouraging²⁴.

The apparent adjustment of the invasive force to the increasing impedance suggests that the pollen tube is able to modulate the force it exerts onto an outside substrate. This is consistent with earlier findings that

describe the modulation of the dilating force in pollen tubes depending on the degree of mechanical constraint¹⁴. It was hypothesized that the modulation of force relies on the modulation of the cell wall mechanical properties and not on that of the turgor pressure. This is consistent with the finding that some pollen tubes burst several minutes after having accomplished the maximum deflection of the micro-cantilever. We hypothesize that these tubes tried to maximize their invasive force by softening the apical cell wall, which eventually became too weak to withhold the turgor pressure and thus burst. This softening of the cell wall could accomplish either or both of two things - reducing the loss of pressure required to deform the cell wall and making it available to act on the cantilever, or allowing the tube to flatten its tip and thus increase the interaction surface with the cantilever. Whether or not this occurs was impossible to determine with statistical certainty in the current set-up since the optics at the interaction region between cantilever and pollen tube could not be imaged at sufficient resolution over time. The immediately adjacent cantilever obscured the interaction surface by causing refraction at its surface.

Very intriguingly, our data showed that upon touching the PDMS cantilever, the peak frequency of oscillation in the pollen tube growth rate was shifted to significantly lower values. Changes in the pollen tube growth dynamics have been related to many environmental conditions such as pH and ion concentration in the medium²⁵⁻²⁸. It is therefore exciting to find evidence that even mechanical triggers are able to influence the growth frequency since this supports the notion of external mechanical resistance being a growth regulating parameter. This is consistent with theoretical models of the oscillating growth that include mechanical factors in the feedback mechanisms postulated to regulate growth^{12,29}. In this model, a rapid growth event triggers mechano-sensitive channels in the apical plasma membrane which cause an influx of calcium into the cytosol. The resulting change in cytosolic calcium influences exocytosis and thus the delivery of new, softer cell wall material to the tip. The apical softening causes a reduction in turgor leading to

water influx and thus a rapid expansion of the tip. An external obstacle would be expected to influence this feedback mechanism as it changes the relationship between the pushing force (hydrostatic pressure) and the resistance posed by the cell wall. Future studies will have to focus on understanding whether the frequency signatures depend on the type of mechanical impedance and the molecular mechanism of mechanosensing in the pollen tube.

Conclusions

This paper successfully developed a multi-layer soft lithography process in order to realize PDMS Lab on Chip monolithically integrated with mechanically compliant PDMS microcantilever for quantifying the invasive growth force of tip growing plant cells, namely, pollen tubes. The developed platforms shows promise for applying to many mechanobiological studies of cells. In this chip called FiLoC, it was possible to harbor growing pollen tubes and direct the elongating apex of the cell through microfluidics channels onto a monolithically integrated PDMS flexure that was flexible enough not to inhibit pollen tube growth without compromising on the measurement of instant growth force of the pollen tubes during the mechanical interactions. The cellular growth force which is measured as 1.5 μN using the deflection of the cantilever and Finite Element Analysis is comparable to other published results.

Acknowledgements

The authors acknowledge research support from *Fonds de Recherche du Québec (FQRNT)* Team Grant to A.G. and M.P. and a Concordia Research Chair to M.P.

References

- 1 A. Sanati Nezhad and A. Geitmann, *Journal of Experimental Botany* 64, 4709-4728 (2013).
- 2 A. Geitmann and R. Palanivelu, *Floriculture and Ornamental Biotechnology* 1, 77-89 (2007).
- 3 O. Gossot and A. Geitmann, *Planta* 226, 405-416 (2007).
- 4 P. Schopfer, *American Journal of Botany* 93, 1415-1425 (2006).
- 5 Y. Chebli and A. Geitmann, *Functional Plant Science and Biotechnology* 1, 232-245 (2007).
- 6 R. Palanivelu and D. Preuss, *Trends in cell biology* 10, 517-524 (2000).

- 7 E. Pierson, D. Miller, D. Callaham, J. Van Aken, G. Hackett and P. Hepler, *Developmental biology* 174, 160-173 (1996).
- 8 R. Zerzour, J. Kroeger and A. Geitmann, *Developmental Biology* 334, 437-446 (2009).
- 9 L. J. Winship, G. Obermeyer, A. Geitmann and P. K. Hepler, *Trends in Plant Science* 15, 363-369 (2010).
- 10 R. Benkert, G. Obermeyer and F.-W. Bentrup, *Protoplasma* 198, 1-8 (1997).
- 11 J. Kroeger and A. Geitmann, *Current opinion in plant biology* 15, 618-624 (2012).
- 12 J. H. Kroeger, R. Zerzour and A. Geitmann, *PloS one* 6, e18549 (2011).
- 13 N. P. Money, *Mycologist* 18, 71-76 (2004).
- 14 A. Sanati Nezhad, M. Naghavi, M. Packirisamy, R. Bhat and A. Geitmann, *Proceedings of the National Academy of Sciences* 110, 8093-8098 (2013).
- 15 C. G. Agudelo, A. Sanati Nezhad, M. Ghanbari, M. Naghavi, M. Packirisamy and A. Geitmann, *The Plant Journal* 73, 1057-1068 (2013).
- 16 M. Ghanbari, A. S. Nezhad, C. G. Agudelo, M. Packirisamy and A. Geitmann, *Journal of bioscience and bioengineering* 117, 504-511 (2014).
- 17 A. Sanati Nezhad, M. Ghanbari, C. G. Agudelo, M. Naghavi, M. Packirisamy, R. B. Bhat and A. Geitmann, *Biomedical Microdevices* 16, 23-33 (2014).
- 18 M. Liu, J. Sun, Y. Sun, C. Bock and Q. Chen, *Journal of Micromechanics and Microengineering* 19, 035028 (2009).
- 19 A. Sanati Nezhad, M. Ghanbari, C. G. Agudelo, M. Packirisamy, R. B. Bhat and A. Geitmann, *IEEE Sensors Journal* 13, 601-609 (2013).
- 20 A. Sanati Nezhad, M. Packirisamy, R. Bhat and A. Geitmann, *IEEE Transactions on Biomedical Engineering* 60, 3185-3193 (2013).
- 21 A. Geitmann, in *Fertilization in Higher Plants*, Springer, 283-302 (1999).
- 22 R. J. Howard, M. A. Ferrari, D. H. Roach and N. P. Money, *Proceedings of the National Academy of Sciences* 88, 11281-11284 (1991).
- 23 J. H. Kroeger, A. Geitmann and M. Grant, *Journal of Theoretical Biology* 253, 363-374 (2008).
- 24 E. Hamilton, G. Jensen, G. Makshev, A. Katims, A. Sherp and E. Haswell, *Science* 350, 438-441 (2015).
- 25 J. A. Feijo, J. Sainhas, T. Holdaway-Clarke, M. S. Cordeiro, J. G. Kunkel and P. K. Hepler, *Bioessays* 23, 86-94 (2001).
- 26 M. A. Messerli, R. Créton, L. F. Jaffe and K. R. Robinson, *Developmental biology* 222, 84-98 (2000).
- 27 M. A. Messerli and K. R. Robinson, *The Plant Journal* 16, 87-91 (1998).
- 28 M. A. Messerli and K. R. Robinson, *Planta* 217, 147-157 (2003).
- 29 J. H. Kroeger and A. Geitmann, *Mathematical Modelling of Natural Phenomena* 8, 25-34 (2013).